International Journal of Engineering, Mathematical and Physical Sciences
ISSN: 2517-9934
Vol:8, No:5, 2014

Stability Analysis of Three-Dimensional Flow and Heat Transfer over a Permeable Shrinking Surface in a Cu-Water Nanofluid

Roslinda Nazar, Amin Noor, Khamisah Jafar, Ioan Pop

***Abstract*—**In this paper, the steady laminar three-dimensional boundary layer flow and heat transfer of a copper (Cu)-water nanofluid in the vicinity of a permeable shrinking flat surface in an otherwise quiescent fluid is studied. The nanofluid mathematical model in which the effect of the nanoparticle volume fraction is taken into account is considered. The governing nonlinear partial differential equations are transformed into a system of nonlinear ordinary differential equations using a similarity transformation which is then solved numerically using the function bvp4c from Matlab. Dual solutions (upper and lower branch solutions) are found for the similarity boundary layer equations for a certain range of the suction parameter. A stability analysis has been performed to show which branch solutions are stable and physically realizable. The numerical results for the skin friction coefficient and the local Nusselt number as well as the velocity and temperature profiles are obtained, presented and discussed in detail for a range of various governing parameters.

***Keywords*—**Heat Transfer, Nanofluid, Shrinking Surface, Stability Analysis, Three-Dimensional Flow.

I. Introduction

NANOFLUIDS are dilute liquid suspensions of nanoparticles with size smaller than ~100nm. Conventional heat transfer fluids such as oil, water, and ethylene glycol mixture are well known as poor heat transfer fluids. Thus, effective thermal conductivity of the nanofluids is expected to enhance the heat transfer performance [1]. The innovative technique, which uses a suspension of nanoparticles in the base fluid, was first introduced by Choi [2] in order to develop advanced heat transfer fluids with substantially higher conductivities. The presence of the nanoparticles in the nanofluid increases the thermal conductivity and therefore, substantially enhances the heat transfer characteristics of the nanofluid. A very good collection of the published papers on nanofluids can be found in the book by Das et al. [3] and in the review papers by Wang and Mujumdar [4]-[6], and Kakaç and Pramuanjaroenkij [7].

R. Nazar is with the School of Mathematical Sciences, Faculty of Science and Technology, UniversitiKebangsaan Malaysia, 43600 UKM Bangi, Selangor, Malaysia (phone: +603–8921-3371; e-mail: rmn@ukm.my).

M.A.M. Noor is with the School of Mathematical Sciences, Faculty of Science and Technology, UniversitiKebangsaan Malaysia, 43600 UKM Bangi, Selangor, Malaysia (e-mail: mamn.ukm@gmail.com).

K. Jafar is with the Faculty of Engineering and Built Environment, Universiti Kebangsaan Malaysia, 43600 UKM Bangi, Selangor, Malaysia (e-mail: kjafar61@gmail.com).

I. Pop is with the Department of Mathematics, Babes-Bolyai University, R-400084 Cluj-Napoca, Romania (e-mail: popm.ioan@yahoo.co.uk).

Many researches on stretching sheet problem have been conducted as mentioned by Miklavcic and Wang [8], Das [9] and Prasad et al. [10]. On the other hand,there isless number of researches in the literature on the shrinking sheet problem. From the consideration of continuity, Crane's stretching sheet solution induced far field suction towards the sheet, while flow over a shrinking sheet would give rise to a velocity away from the sheet [8], [10]. From a physical point of view, vorticity generated at the shrinking sheet is not confined within a boundary layer and a steady flow is unlikely to exist unless adequate suction on the surface is imposed [8], [10].

In this paper, we extend the shrinking sheet problem to a three-dimensional space in Cu-water nanofluid. The purpose of this paper is to study the properties of the flow and heat transfer due to a shrinking sheet with suction. Using appropriate similarity variables, the partial differential equations are transformed into ordinary differential equations and then are solved numerically. Since dual solutions are found for some range of parameters value, a stability analysis is performed in order to determine which solution is physically realizable. To the best of our knowledge, the stability analysis of the present problem has not been considered before and thus the reported results are original and new.

II. Governing Equations

We consider the three dimensional boundary layer flow of a Cu-water nanofluid in the vicinity of a permeable shrinking flat surface in an otherwise quiescent fluid. It is assumed that the nanofluid is incompressible and the flow is laminar. A locally orthogonal set of coordinates (x,y,z) is chosen with the origin O in the plane of the shrinking sheet. The x- and y- coordinates are in the plane of the shrinking sheet, while the coordinate z is measured in the perpendicular direction to the shrinking surface as shown in Fig. 1. It is assumed that the flat surface is shrinking continuously in both the x- and y-directions with the velocities $u_w(x)=a\,x$ and $v_w(y)=b\,y$, respectively, where a and b are negative constants. It is also assumed that the surface temperature is T_w and the ambient temperature is T_∞ where T_w and T_∞ are constants, with $T_w > T_\infty$. The nanofluid is the suspension of solid particles in nano-scale in a base fluid. The nanoparticles considered here is copper, Cu, and the base fluid is water. The thermophysical properties of the base fluid and the nanoparticles are given in Table I.

Using the mathematical model for nanofluids proposed by Tiwari and Das [11], the governing equations are given by

$$\frac{\partial u}{\partial x}+\frac{\partial v}{\partial y}+\frac{\partial w}{\partial z}=0 \tag{1}$$

$$\frac{\partial u}{\partial t}+u\frac{\partial u}{\partial x}+v\frac{\partial u}{\partial y}+w\frac{\partial u}{\partial z}=\frac{\mu_{\rm nf}}{\rho_{\rm nf}}\frac{\partial^2 u}{\partial z^2} \tag{2}$$

$$\frac{\partial v}{\partial t}+u\frac{\partial v}{\partial x}+v\frac{\partial v}{\partial y}+w\frac{\partial v}{\partial z}=\frac{\mu_{\rm nf}}{\rho_{\rm nf}}\frac{\partial^2 v}{\partial z^2} \tag{3}$$

$$\frac{\partial T}{\partial t}+u\frac{\partial T}{\partial x}+v\frac{\partial T}{\partial y}+w\frac{\partial T}{\partial z}=\alpha_{\rm nf}\frac{\partial^2 T}{\partial z^2} \tag{4}$$

subject to the initial and boundary conditions

$$\begin{aligned} &t<0:\ u=0,\ v=0,\ w=0,\ T=T_\infty \ \text{ for any } x,\ y,\ z\\ &t\geq 0:\ u=\lambda u_w(x)=\lambda a x,\quad v=\lambda v_w(y)=\lambda b y,\\ &\qquad w=w_0,\quad T=T_w \quad \text{at} \quad z=0\\ &\qquad u\to 0,\quad v\to 0,\quad T\to T_\infty \quad \text{as} \quad z\to\infty \end{aligned} \tag{5}$$

Here u, v and w are the velocity components along the $x-$, $y-$ and $z-$ axes, respectively, w_0 is the mass velocity with $w_0<0$ for suction and $w_0>0$ for injection, T is the temperature of the nanofluid and λ is the shrinking parameter. Further, $\mu_{\rm nf}$, $\rho_{\rm nf}$ and $\alpha_{\rm nf}$ are the effective viscosity, the effective density and the effective thermal diffusivity ofthe nanofluid, which are defined as (see [12])

$$\begin{aligned} &\mu_{\rm nf}=\frac{\mu_{\rm f}}{(1\text{-}\phi)^{2.5}},\quad \alpha_{\rm nf}=\frac{k_{\rm nf}}{(\rho {\rm C_p})_{\rm nf}},\\ &(\rho C_p)_{\rm nf}=(1-\phi)(\rho C_p)_{\rm f}+\phi(\rho C_p)_s,\\ &\frac{k_{\rm nf}}{k_{\rm f}}=\frac{(k_{\rm s}+2k_{\rm f})-2\phi(k_{\rm f}-k_{\rm s})}{(k_{\rm s}+2k_{\rm f})+\phi(k_{\rm f}-k_{\rm s})} \end{aligned} \tag{6}$$

where ϕ is the solid volume fraction of the nanofluid, $(\rho C_p)_{\rm nf}$ is the heat capacitance of the nanofluid, $k_{\rm nf}$ is the effective thermal conductivity of the nanofluid and the subscript '*nf*' represents the nanofluid, '*f*' represents the base fluid and '*s*' represents the solid or nanoparticles. The expression of $\mu_{\rm nf}$ has been proposed by Brinkman [13]. It is worth mentioning that (6) is restricted to spherical nanoparticles where it does not account for other shapes of nanoparticles. Other models for the effective thermal conductivity of the nanofluid, $k_{\rm nf}$ can be found, for example, in the paper by Ding et al. [14].

III. Steady-State Flow Case

We introduce now the following similarity variables:

$$\begin{aligned} &u=a x f'(\eta),\quad v=b y g'(\eta),\quad w=-(a\nu_f)^{1/2}(f+cg)\\ &\theta(\eta)=(T-T_\infty)/(T_w-T_\infty),\quad \eta=(a/\nu_f)^{1/2}z \end{aligned} \tag{7}$$

where primes denote differentiation with respect to η and $\nu_{\rm f}$ is the kinematic viscosity of the base fluid. Substituting the similarity variables (7) into (1)-(4), it is found that the continuity (1) is automatically satisfied, and (2)-(4) are reduced to

$$\varepsilon_1 f'''+(f+cg)f''-f'^2=0 \tag{8}$$

$$\varepsilon_1 g'''+(f+cg)g''-g'^2=0 \tag{9}$$

$$\frac{\varepsilon_2}{\rm Pr}\theta''+(f+cg)\theta'=0 \tag{10}$$

and the boundary conditions (5) become

$$\begin{aligned} &f(0)=s,\ f'(0)=\lambda,\ g(0)=0,\ g'(0)=\lambda,\ \theta(0)=1\\ &f'(\eta)\to 0,\quad g'(\eta)\to 0,\quad \theta(\eta)\to 0 \quad \text{as} \quad \eta\to\infty \end{aligned} \tag{11}$$

Here ${\rm Pr}=\nu_{\rm f}/\alpha_{\rm f}$ is the Prandtl number, $c=b/a$ is the ratio of the surface velocity gradients along the y- and x-directions, s is the suction parameter, and ε_1 and ε_2 are two constants relating to the properties of the nanofluid, defined by

$$\begin{aligned} &\varepsilon_1=\frac{1}{(1-\phi)^{2.5}\left(1-\phi+\phi\rho_{\rm s}/\rho_{\rm f}\right)},\\ &\varepsilon_2=\frac{k_{\rm nf}/k_{\rm f}}{(1-\phi)+\phi(\rho C_{\rm p})_{\rm s}/(\rho C_{\rm p})_{\rm f}} \end{aligned} \tag{12}$$

It is worth mentioning that for $s=0$ (impermeable surface) and $c=0$ (plane shrinking sheet), (8)-(10) reduce to

$$\varepsilon_1 f'''+ff''-f'^2=0 \tag{13}$$

$$\frac{\varepsilon_2}{\rm Pr}\theta''+f\theta'=0 \tag{14}$$

subject to

$$\begin{aligned} &f(0)=0,\quad f'(0)=\lambda,\quad \theta(0)=1\\ &f'(\eta)\to 0,\quad \theta(\eta)\to 0 \quad \text{as} \quad \eta\to\infty \end{aligned} \tag{15}$$

However, for $s=0$ (impermeable surface) and $c=1$ (axisymmetric shrinking sheet), (8)-(10) reduce to

$$\varepsilon_1 f'''+2ff''-f'^2=0 \tag{16}$$

$$\frac{\varepsilon_2}{\rm Pr}\theta''+2f\theta'=0 \tag{17}$$

with the boundary conditions (15). Therefore, we will confine our attention here only to the case when $0\leq c\leq 1$.

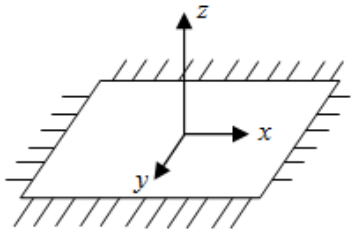

Fig. 1 Physical model and coordinate system

The physical quantities of practical interest are the local skin friction coefficients C_{fx} and C_{fy} and the local Nusselt number Nu_x, which are defined as

$$C_{fx}=\frac{\tau_{wx}}{\rho_f u_w^2},\quad C_{fy}=\frac{\tau_{wy}}{\rho_f v_w^2},\quad Nu_x=\frac{x q_w}{k_f (T_w-T_\infty)} \tag{18}$$

where τ_{wx} and τ_{wy} are the shear stresses in the x- and y-directions, respectively, and q_w is the heat flux from the surface of the shrinking sheet, which are given by

$$\tau_{wx}=\mu_{nf}\left(\frac{\partial u}{\partial z}\right)_{z=0},\quad \tau_{wy}=\mu_{nf}\left(\frac{\partial v}{\partial z}\right)_{z=0},\quad q_w=-k_{nf}\left(\frac{\partial T}{\partial z}\right)_{z=0} \tag{19}$$

Substituting (7) into (18) and using (19), we obtain

$$\begin{aligned}&\mathrm{Re}_x^{1/2} C_{fx}=\frac{f''(0)}{(1-\phi)^{2.5}},\quad \mathrm{Re}_y^{1/2} C_{fy}=\frac{g''(0)}{(1-\phi)^{2.5}},\\ &\mathrm{Re}_x^{-1/2} Nu_x=-\frac{k_{nf}}{k_f}\theta'(0)\end{aligned} \tag{20}$$

where $\mathrm{Re}_x=u_w(x)x/\nu_f$ and $\mathrm{Re}_y=v_w(y)y/\nu_f$ are the local Reynolds numbers based on the velocities $u_w(x)$ and $v_w(y)$, respectively.

TABLE I
THERMOPHYSICAL PROPERTIES OF FLUID AND NANOPARTICLES [a]

Physical properties	Fluid phase(water)	Cu (Copper)
C_p (J/kg K)	4179	385
ρ (kg/m^3)	997.1	8933
k (W/mK)	0.613	400
$\alpha \times 10^7$ (m^2/s)	1.47	11163.1
$\beta \times 10^{-5}$ (1/K)	21	1.67

[a] Oztop and Abu-Nada [12]

IV. STABILITY ANALYSIS

It has been shown in some papers ([16] or [17]) that dual (lower and upper branch) solutions exist. In order to determine which of these solutions are physically realizable in practice, a stability analysis of (8)-(11) is necessary. Following Weidman et al. [16], a dimensionless time variable τ has to be introduced. The use of τ is associated with an initial value problem and this is consistent with the question of which solution will be obtained in practice (physically realizable). Thus, the new variables for the unsteady problem are

$$\begin{aligned}&u=ax\frac{\partial f(\eta,\tau)}{\partial \eta},\ v=by\frac{\partial g(\eta,\tau)}{\partial \eta},\ w=-(a\nu_f)^{1/2}\left[f(\eta,\tau)+cg(\eta,\tau)\right]\\ &\theta(\eta,\tau)=(T-T_\infty)/(T_w-T_\infty),\ \eta=(a/\nu_f)^{1/2}z,\ \tau=at\end{aligned} \tag{21}$$

Substituting (21) into (2)-(4), we obtain

$$\varepsilon_1\frac{\partial^3 f}{\partial \eta^3}+(f+cg)\frac{\partial^2 f}{\partial \eta^2}-\left(\frac{\partial f}{\partial \eta}\right)^2-\frac{\partial^2 f}{\partial \eta\,\partial \tau}=0 \tag{22}$$

$$\varepsilon_1\frac{\partial^3 g}{\partial \eta^3}+(f+cg)\frac{\partial^2 g}{\partial \eta^2}-\left(\frac{\partial g}{\partial \eta}\right)^2-\frac{\partial^2 g}{\partial \eta\,\partial \tau}=0 \tag{23}$$

$$\frac{\varepsilon_2}{\mathrm{Pr}}\frac{\partial^2 \theta}{\partial \eta^2}+(f+cg)\frac{\partial \theta}{\partial \eta}-\frac{\partial \theta}{\partial \tau}=0 \tag{24}$$

subject to the boundary conditions

$$\begin{aligned}&f(0,\tau)=s,\ \frac{\partial f}{\partial \eta}(0,\tau)=\lambda,\ g(0,\tau)=0,\ \frac{\partial g}{\partial \eta}(0,\tau)=\lambda,\ \theta(0,\tau)=1\\ &\frac{\partial f}{\partial \eta}(\eta,\tau)\to 0,\ \frac{\partial g}{\partial \eta}(\eta,\tau)\to 0,\ \theta(\eta,\tau)\to 0 \text{ as } \eta\to\infty\end{aligned} \tag{25}$$

To determine the stability of the solution $f=f_0(\eta),\ g=g_0(\eta)$ and $\theta=\theta_0(\eta)$ satisfying the boundary-value problem (8)-(11), we write (see [16] or [17])

$$\begin{aligned}f(\eta,\tau)&=f_0(\eta)+e^{-\gamma\tau}F(\eta,\tau),\\ g(\eta,\tau)&=g_0(\eta)+e^{-\gamma\tau}G(\eta,\tau),\\ \theta(\eta,\tau)&=\theta_0(\eta)+e^{-\gamma\tau}S(\eta,\tau),\end{aligned} \tag{26}$$

where γ is an unknown eigenvalue parameter, and $F(\eta,\tau)$, $G(\eta,\tau)$ and $S(\eta,\tau)$ are small relative to $f_0(\eta)$, $g_0(\eta)$ and $\theta_0(\eta)$. Substituting (26) into (22)-(24), we obtain the following linearized problem:

$$\varepsilon_1\frac{\partial^3 F}{\partial \eta^3}+(f_0+cg_0)\frac{\partial^2 F}{\partial \eta^2}+(F+cG)f_0''-2f_0'\frac{\partial F}{\partial \eta}+\gamma\frac{\partial F}{\partial \eta}-\frac{\partial^2 F}{\partial \eta\,\partial \tau}=0 \tag{27}$$

$$\varepsilon_1\frac{\partial^3 G}{\partial \eta^3}+(f_0+cg_0)\frac{\partial^2 G}{\partial \eta^2}+(F+cG)g_0''-2cg_0'\frac{\partial G}{\partial \eta}+\gamma\frac{\partial G}{\partial \eta}-\frac{\partial^2 G}{\partial \eta\,\partial \tau}=0 \tag{28}$$

$$\frac{\varepsilon_2}{\mathrm{Pr}}\frac{\partial^2 S}{\partial \eta^2}+(f_0+cg_0)\frac{\partial S}{\partial \eta}+(F+cG)\theta_0'+\gamma S-\frac{\partial S}{\partial \tau}=0 \tag{29}$$

subject to the boundary conditions

$$\begin{aligned}&F(0,\tau)=0,\ \frac{\partial F}{\partial \eta}(0,\tau)=0,\ G(0,\tau)=0,\ \frac{\partial G}{\partial \eta}(0,\tau)=0,\ S(0,\tau)=0\\ &\frac{\partial F}{\partial \eta}(\eta,\tau)\to 0,\ \frac{\partial G}{\partial \eta}(\eta,\tau)\to 0,\ S(\eta,\tau)\to 0 \text{ as } \eta\to\infty\end{aligned} \tag{30}$$

As suggested by Weidman et al. [16], we investigate the stability of the steady flow and heat transfer solution $f_0(\eta)$, $g_0(\eta)$ and $\theta_0(\eta)$ by setting $\tau = 0$, and hence $F = F_0(\eta)$, $G = G_0(\eta)$ and $S = S_0(\eta)$ in (26)-(28) to identify initial growth or decay of the solution (25). To test our numerical procedure we have to solve the linear eigenvalue problem:

$$\varepsilon_1 F_0''' + (f_0 + c g_0) F_0'' + (F_0 + c G_0) f_0'' + (\gamma - 2 f_0') F_0' = 0 \quad (31)$$

$$\varepsilon_1 G_0''' + (f_0 + c g_0) G_0'' + (F_0 + c G_0) g_0'' + (\gamma - 2c g_0') G_0' = 0 \quad (32)$$

$$\frac{\varepsilon_2}{\Pr} S_0'' + (f_0 + c g_0) S_0' + (F_0 + c G_0) \theta_0' + \gamma S_0 = 0 \quad (33)$$

with the boundary conditions

$$\begin{aligned} &F_0(0) = 0,\ F_0'(0) = 0,\ G_0(0) = 0,\ G_0'(0) = 0,\ S_0(0) = 0 \\ &F_0'(\eta) \to 0,\ G_0'(\eta) \to 0,\ S_0(\eta) \to 0 \text{ as } \eta \to \infty \end{aligned} \quad (34)$$

It should be mentioned that for particular values of λ, s and c, the corresponding steady flow solution $f_0(\eta)$, $g_0(\eta)$ and $\theta_0(\eta)$, the stability of the steady flow solution is determined by the smallest eigenvalue γ_1. According to Harris et al. [18], the range of possible eigenvalues can be determined by relaxing a boundary condition on $F_0'(\eta)$, $G_0'(\eta)$ or $S_0(\eta)$. For the present problem, we relax the condition that $G_0'(\eta) \to 0$ as $\eta \to \infty$ and for a fixed value of γ we solve the system (31-33) along with the new boundary condition $G_0''(0) = 1$.

V. Results and Discussion

The system of nonlinear ordinary differential equations (8), (9) and (10) subject to the boundary conditions (11) was solved numerically using the function bvp4c in Matlab for different values of the nanoparticle volume fraction ϕ, suction parameter s andsurface velocity gradients ratio c. Following Oztop and Abu-Nada [12], the Prandtl number Pr is set equal to 6.2 (water) and the range of nanoparticle volume fraction is considered as $0 \le \phi \le 0.2$, in which $\phi = 0$ corresponds to the regular base fluid. The dual (first and second) solutions are obtained by setting different initial guesses for the missing values of $f''(0)$, $g''(0)$, and $\theta'(0)$, where all profiles satisfy the far field boundary conditions (11) asymptotically. The effects of the nanoparticle volume fraction ϕ, suction parameter s, surface velocity gradients ratio c, and the Prandtl number Pr on the skin friction coefficient, Nusselt number, velocity profiles and temperature profiles are analyzed for the Cu–water nanofluid. Since the present problem has more than one solution (dual solutions), the bvp4c function requires an initial guess which should satisfy the boundary conditions and reveals the behavior of the desired solution. While it is easy to find the first (upper branch) solution even using a poor initial guess, it is very difficult however to find the second (lower branch) solution. To overcome this difficulty, we begin with a set of parameter values for which the problem is easy to be solved. The obtained results are then used as initial guess for the solution of the problem with small variation of the parameters. This step is repeated until the desired values of parameters are reached. This technique is called continuation [19], [20].

TABLE II
Comparison of Reduced Skin-Friction Coefficient and Reduced Nusselt Number for Some Values of c [a]

c	Upper Branch			Lower Branch		
	f''(0)	g''(0)	(-)θ'(0)	f''(0)	g''(0)	–θ'(0)
0.0	2.5290 [2.5290]	- [-]	6.8225 [6.8225]	0.5847 [0.5847]	- [-]	6.6931 [6.6931] [a]
0.2	2.4444	2.7061	6.7371	0.7165	2.4073	6.6086
0.5	2.2885	2.4777	6.5946	0.9764	2.1097	6.4708
0.8	2.0403	2.1404	6.4172	1.4444	1.7315	6.3254

[a]Rohni et al. [15]

In order to validate our numerical results, a comparison of the reduced skin friction coefficient and the reduced Nusselt number has been made as shown in Table II when $\lambda = -1$, s=2.1, and $\phi = 0.2$. The present results shows an excellent agreement with those reported by Rohni et al. [15],thus gives us confidence on the accuracy of our numerical results presented in this paper. Figs. 2 to 10 show the existence of dual solutions for the shrinking sheet problem. The solution exists up to some critical value of λ, say λ_c, beyond which the boundary layer separates from the surface and the solution based upon the boundary-layer approximations are not possible. Some values of λ_c are presented in Table III for various values of ϕ, s and c. It can be seen that the absolute value of λ_c increases with the increase of nanoparticle volume fraction parameter ϕ and suction parameter$s$, while it decreases with the increase of surface velocity gradient ratio.

TABLE III
The Values of λ_c for Various Values of ϕ, s and c

ϕ	s	c	λ_c
0	2.1	0.5	-0.8326
0.05	2.1	0.5	-1.0239
0.1	2.1	0.5	-1.1490
0.2	2.1	0.2	-1.4585
0.2	2.1	0.5	-1.2353
0.2	2.1	0.8	-1.0528
0.2	2.3	0.5	-1.4817
0.2	2.5	0.5	-1.7507
0.2	2.7	0.5	-2.0420

The variations of the reduced skin friction coefficient $f''(0)$ and $g''(0)$ with λ are shown in Figs. 2-7 for which the effect of parameter ϕ, s and c are investigated. It can be seen that the skin friction coefficient increases with nanoparticle volume fraction and suction parameter. Physically this means increasing the magnitude of ϕ and s will consequently increases the heat transfer rate at the surface. On the other hand, the reverse effect occurs when the surface velocity

gradient ratio increases. As seen from the figures, the values of $f''(0)$ and $g''(0)$ are always positive (for all the first solution) when $\lambda < 0$ until some critical value λ_c. A positive sign for $f''(0)$ and $g''(0)$ implies that the fluid exerts a drag force on the plate while a negative sign implies the opposite.

Figs. 8-10 illustrate the variations of the reduced Nusselt number $-\theta'(0)$ with λ due to the effect of the nanoparticle volume fraction ϕ, suction parameter *s*, and surface velocity gradient ratio *c,* respectively, when default parameter values are fixed as ϕ=0.2, *s*=2.1, and *c*=0.5, unless stated otherwise. From these figures, the nanoparticle volume fraction parameter gives the most significant effect on the reduced Nusselt number, while the surface velocity gradient ratio is the less significant factor.

The samples of velocity and temperature profiles are presented in Figs. 11-13. These profiles have essentially the same form as in the case of regular fluid $(\phi = 0)$. Figs.11-13 show that the far field boundary conditions (11) are satisfied asymptotically, thus support the validity of the numerical results, besides supporting the existence of the dual solutions shown in Figs. 2-10.

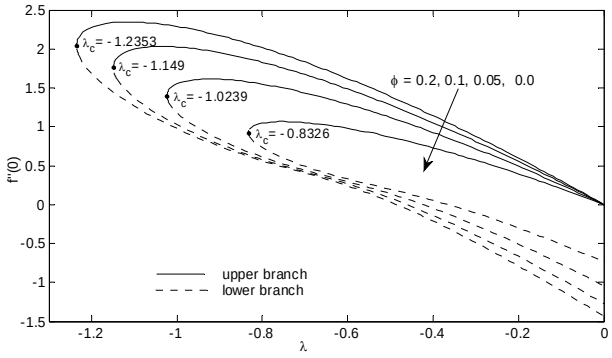

Fig. 2 Variation of $f''(0)$ with λ for different values of ϕ when $s = 2.1$ and $c = 0.5$

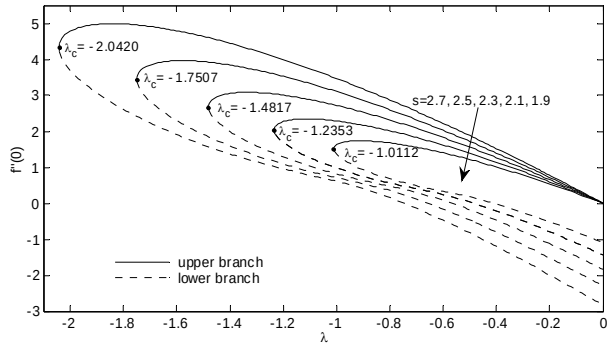

Fig. 3 Variation of $f''(0)$ with λ for different values of *s* when $\phi = 0.2$ and $c = 0.5$

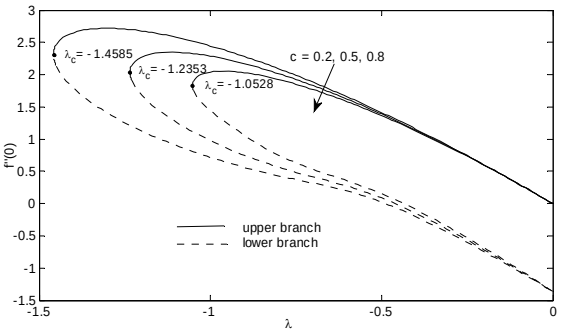

Fig. 4 Variation of $f''(0)$ with λ for different values of *c* when $\phi = 0.2$ and $s = 2.1$

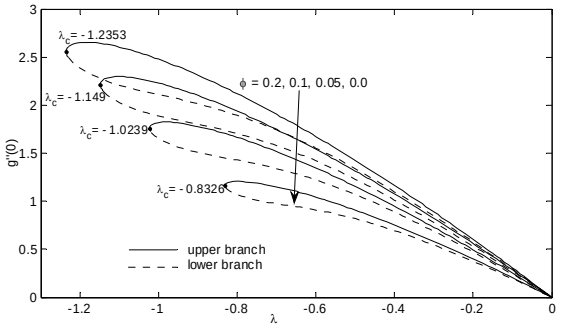

Fig. 5 Variation of $g''(0)$ with $\lambda$for different values of ϕ when $s = 2.1$ and $c = 0.5$

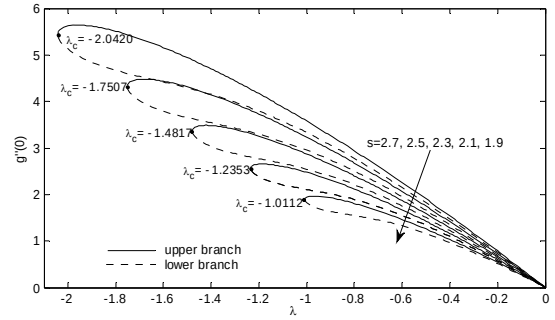

Fig. 6 Variation of $g''(0)$ with λ for different values of *s* when $\phi = 0.2$ and $c = 0.5$

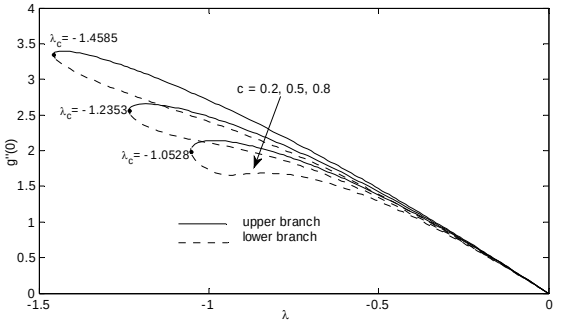

Fig. 7 Variation of $g''(0)$ with λ for different values of *c* when $\phi = 0.2$ and $s = 2.1$

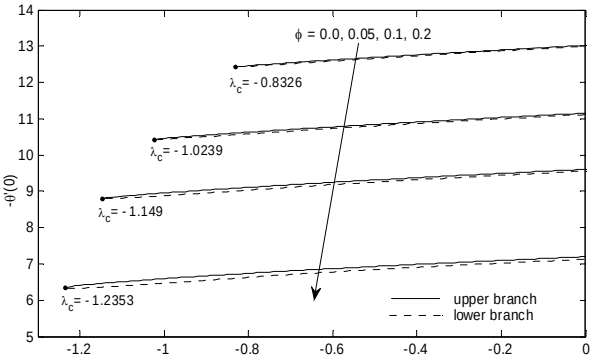

Fig. 8 Variation of $-\theta'(0)$ with λ for different values of ϕ when $s = 2.1$ and $c = 0.5$

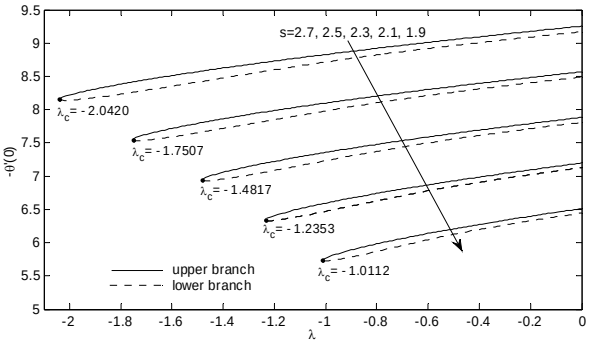

Fig. 9 Variation of $-\theta'(0)$ with λ for different values of s when $\phi = 0.2$ and $c = 0.5$

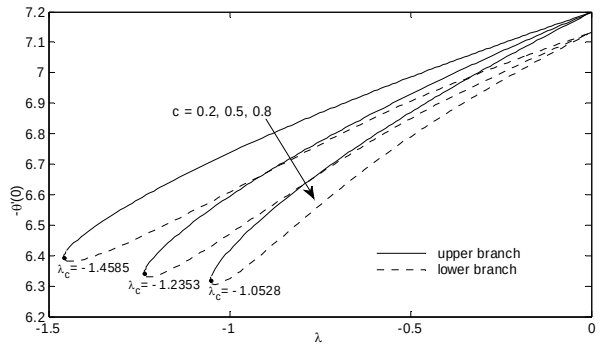

Fig. 10 Variation of $-\theta'(0)$ with λ for different values of c when $\phi = 0.2$ and $s = 2.1$

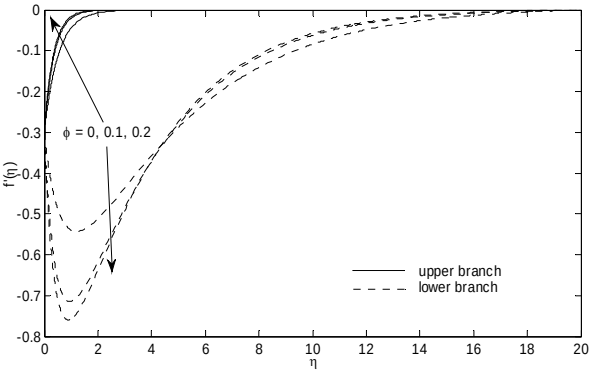

Fig. 11 Velocity profiles $f'(\eta)$ for some value of nanoparticle volume fraction ϕ

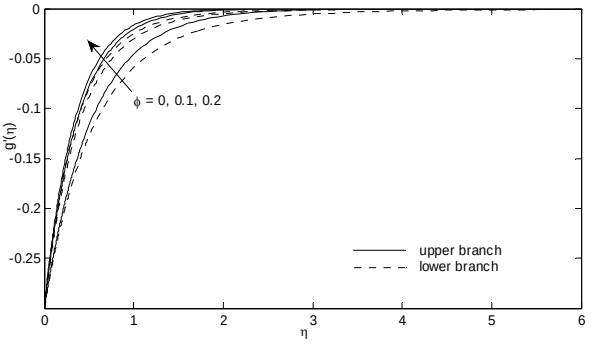

Fig. 12 Velocity profiles $g'(\eta)$ for some value of nanoparticle volume fraction ϕ

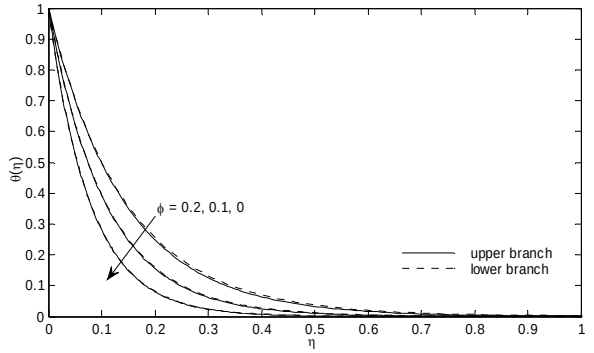

Fig. 13 Temperature profiles $\theta(\eta)$ for some value of nanoparticle volume fraction ϕ

A stability analysis is performed using bvp4c in Matlab to determine which solution is more stable. Numerical solutions obtained from the steady ordinary differential equation (8)–(10) need to be used while solving the linear eigenvalue problem (31)–(33). The smallest eigenvalue γ_1 for some values of s and λ are shown in Table IV when ϕ=0.2 and c=0.5. The results show that all the upper branch solutions have positive eigenvalue γ_1 while all the lower branch solutions have negative eigenvalue γ_1. We conclude that the

upper branch solution is stable while the lower branch is unstable over time. Notice that as λ approaches critical value λ_c, the smallest eigenvalue becomes closer to zero. In fact the eigenvalue signs changed from positive to negative at the turning point of the upper and lower branch.

TABLE IV
SMALLEST EIGENVALUE γ_1 FOR SOME VALUES OF S

s	λ	γ_1 (upper branch)	γ_1 (lower branch)
2.1	1	0.7522	-0.5014
	1.2	0.2884	-0.2497
	1.23	0.1088	-0.1029
2.3	1	1.156	-0.6412
	1.4	0.4855	-0.3967
	1.48	0.0687	-0.0667
2.5	1	1.5481	-0.7283
	1.5	0.9254	-0.6597
	1.7	0.4114	-0.3561
	1.75	0.0466	-0.0458

VI. CONCLUSION

We have studied numerically the problem of steady three dimensional boundary-layer flow of a Cu-water nanofluid past a permeable shrinking surface. The governing partial differential equations are transformed into ordinary differential equations by similarity transformation and then are solved numerically using bvp4c in Matlab. The comparison of the results with previously published results show an excellent agreement thus gives us confidence in our computations presented in this paper. Numerical results for the reduced skin-friction coefficient and the local Nusselt number as well as the velocity and temperature profiles are illustrated in tables and graphs for some values of parameters. Dual solutions are found for this shrinking sheet problem. The stability analysis is performed and shows that the upper branch solution is stable while the lower branch solution is unstable.

ACKNOWLEDGMENT

This work was supported by the research grants (DIP-2012-31 and GUP-2013-040) from the Universiti Kebangsaan Malaysia.

REFERENCES

[1] H. Masuda, A. Ebata, K. Teramea and N. Hishinuma, NetsuBussei, 4 (4), 227-233 (1993).
[2] S.U.S. Choi, ASME Fluids Eng. Division, 231, 99–105 (1995).
[3] S.K. Das, S.U.S. Choi, W. Yu and T. Pradeep, Nanofluids: Science and Technology, New Jersey: Wiley, 2007.
[4] X.-Q Wang and A.S. Mujumdar, Int. J. Thermal Sci., 46, 1-19 (2007).
[5] X.-Q. Wang and A.S. Mujumdar, Brazilian J. Chem. Engng., 25, 613-630 (2008).
[6] X.-Q. Wang and A.S. Mujumdar, Brazilian J. Chem. Engng., 25 631-648 (2008).
[7] S. Kakaç and A. Pramuanjaroenkij, Int. J. Heat Mass Transfer, 52, 3187-3196 (2009).
[8] M. Miklavčič and C.Y. Wang, Viscous flow due to a shrinking sheet. Quart. Appl. Math. 46 (2006) 283-290.
[9] K. Das, Computer and Fluids, 64, 34-42 (2012).
[10] K. V. Prasad, K. Vajravelu and I. Pop, Int. J. of Applied Mechanics and Engineering, 18 (3), 779-791 (2013).
[11] R.K. Tiwari and M.K. Das, Int. J. Heat Mass Transfer, 50, 2002-2018 (2007).
[12] H.F. Oztop and E. Abu-Nada, Int. J. Heat Fluid Flow, 29, 1326-1336 (2008).
[13] H.C. Brinkman, J. Chem. Phys. 20, 571–581 (1952).
[14] Y. Ding, H. Chen, L. Wang, C. Y. Yang, Y. He, W. Yang, W. P. Lee, L. Zhang and R. Huo, KONA, 25, (2007).
[15] A.M. Rohni, S. Ahmad and I. Pop, Int. J. Heat Mass Transfer, 55, 1888-1895 (2012).
[16] P.D. Weidman, D.G. Kubittschek, A.M.J. Davis, The effect of transpiration on self-similar boundary layer flow over moving surfaces. Int. J. Engng. Sci. 44 (2006) 730-737.
[17] A.V. Roşca, I. Pop, Flow and heat transfer over a vertical permeable stretching/shrinking sheet with a second order slip. Int. J. Heat Mass Transfer 60 (2013) 355-364.
[18] S.D. Harris, D.B. Ingham, I. Pop, Mixed convection boundary-layer flow near the stagnation point on a vertical surface in a porous medium: Brinkman model with slip, Transport Porous Media 77 (2009) 267-285.
[19] L.F. Shampine, I. Gladwell, S. Thompson, Solving ODEs with MATLAB, Cambridge University Press, 2003.
[20] L.F. Shampine, M.W. Reichelt, J. Kierzenka, Solving boundary value problems for ordinary differential equations in Matlab with bvp4c, 2010. <http://www.mathworks.com/ bvp tutorial>.